

# Autologous Breast Reconstruction: Preoperative Magnetic Resonance Angiography for Perforator Flap Vessel Mapping

Mukta D. Agrawal, MD<sup>1</sup> Nanda Deepa Thimmappa, MD<sup>2</sup> Julie V. Vasile, MD<sup>3,4</sup> Joshua L. Levine, MD<sup>3</sup>  
Robert J. Allen, MD<sup>3</sup> David T. Greenspun, MD<sup>3</sup> Christina Y. Ahn, MD<sup>5</sup> Constance M. Chen, MD<sup>6</sup>  
Sandeep S. Hedgire, MD<sup>1</sup> Martin R. Prince, MD, PhD<sup>2</sup>

<sup>1</sup> Department of Radiology, Massachusetts General Hospital Imaging, Boston, Massachusetts

<sup>2</sup> Department of Radiology, Weill Cornell Imaging at NewYork Presbyterian Hospital, New York

<sup>3</sup> Department of Microsurgery, New York Eye and Ear Infirmary, New York

<sup>4</sup> Department of Plastic Surgery, Northern Westchester Hospitals, New York

<sup>5</sup> Department of Plastic Surgery, NYU Langone Medical Center, New York

<sup>6</sup> NewYork-Presbyterian Hospital, Columbia University, New York

Address for correspondence Mukta D. Agrawal, MD, Department of Radiology, Massachusetts General Hospital Imaging, 846 Massachusetts Avenue, Apt.3D, Arlington, MA 02476 (e-mail: mukta.dr@gmail.com).

J Reconstr Microsurg 2015;31:1–11.

## Abstract

**Background** Selection of a vascular pedicle for autologous breast reconstruction is time consuming and depends on visual evaluation during the surgery. Preoperative imaging of donor site for mapping the perforator artery anatomy greatly improves the efficiency of perforator selection and significantly reduces the operative time. In this article, we present our experience with magnetic resonance angiography (MRA) for perforator vessel mapping including MRA technique and interpretation.

**Methods** We have performed over 400 MRA examinations from August 2008 to August 2013 at our institution for preoperative imaging of donor site for mapping the perforator vessel anatomy. Using our optimized imaging protocol with blood pool magnetic resonance imaging contrast agents, multiple donor sites can be imaged in a single MRA examination. Following imaging using the postprocessing and reporting tool, we estimated incidence of commonly used perforators for autologous breast reconstruction.

**Results** In our practice, anterior abdominal wall tissue is the most commonly used donor site for perforator flap breast reconstruction and deep inferior epigastric artery perforators are the most commonly used vascular pedicle. A thigh flap, based on the profunda femoral artery perforator has become the second most used flap at our institution. In addition, MRA imaging also showed evidence of metastatic disease in 4% of our patient subset.

**Conclusion** Our MRA technique allows the surgeons to confidently assess multiple donor sites for the best perforator and flap design. In conclusion, a well-performed MRA with specific postprocessing provides an accurate method for mapping perforator vessel, at the same time avoiding ionizing radiation.

## Keywords

- ▶ MRA
- ▶ blood pool contrast agent
- ▶ perforator flap artery imaging

received  
October 1, 2013  
accepted after revision  
January 19, 2014  
published online  
May 29, 2014

Copyright © 2015 by Thieme Medical Publishers, Inc., 333 Seventh Avenue, New York, NY 10001, USA.  
Tel: +1(212) 584-4662.

DOI <http://dx.doi.org/10.1055/s-0034-1372475>.  
ISSN 0743-684X.

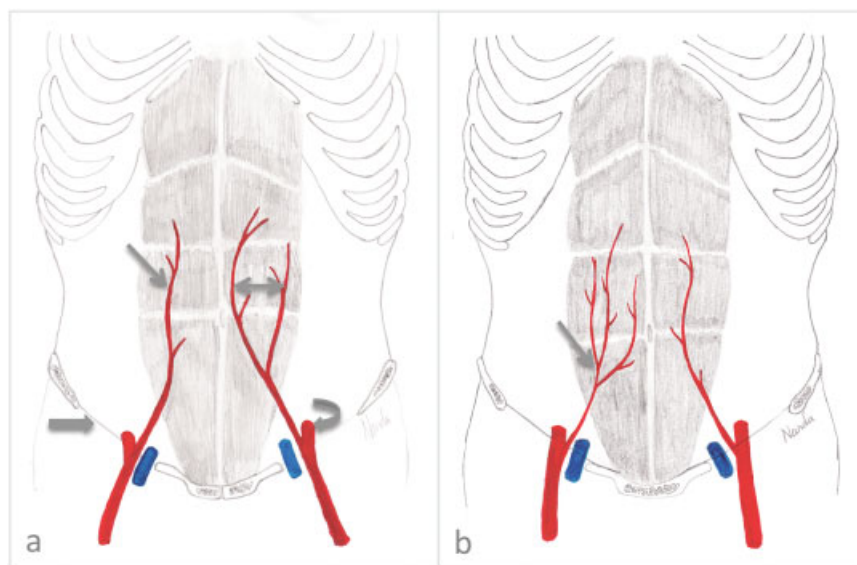


**Fig. 1** (a, b) Diagrammatic illustration (frontal view) demonstrates the origin and branching patterns of the deep inferior epigastric artery (DIEA), which arises from the external iliac artery (curved arrow in [a]) just above the inguinal ligament (block arrow in [a]). From there the DIEA courses upward in one of the three branching patterns: a single trunk (straight arrow in [a]), bifurcating into medial and lateral branches (double head arrow in [a]), or subdividing into three or more branches (straight arrow in [b]).

Breast cancer is the most common cancer worldwide, and causes the most cancer-related deaths among women worldwide.<sup>1</sup> Surgical breast reconstruction after mastectomy is a vital component of the overall breast cancer treatment plan. The goal of reconstruction is to restore breast symmetry and improve quality of life without affecting the prognosis or detection of recurrence as well as offering psychological benefit of alleviating the feeling of deformity following mastectomy, thus eliminating a constant reminder of disease.<sup>2</sup>

Autologous breast reconstruction involves tissue transfer from a donor site on the patient's own body along with its native vasculature such that the reconstructed breast closely resembles normal breast. Autologous reconstruction comes in various forms, including pedicled, free, and perforator flaps. The traditional myocutaneous flap (latissimus dorsi flap and transverse rectus abdominis muscle flap) involves transfer of muscle along with skin and subcutaneous fat to create a breast mound. These muscle sacrificing flaps are associated with donor site morbidity including abdominal wall laxity and weakness.<sup>3,4</sup>

Perforator flap breast reconstruction involves transfer of autologous skin and subcutaneous fat with its supplying artery/vein bundle: the perforators. Perforator flap breast reconstruction requires specialized surgical expertise and many hours of operative time to first harvest the graft and then reconstruct the breast. Preoperative imaging of donor site with computed tomography (CT)/magnetic resonance (MR) angiography provides a perforator roadmap to facilitate surgical planning, reduce operative time and complications, and improve the patient outcomes.<sup>5-7</sup>

The article describes relevant anatomy of commonly used donor sites and a detailed account of acquisition and interpretation of the preferred MRA approach based upon our experience in over 400 cases.

## Relevant Anatomy

### Deep and Superficial Inferior Epigastric Arteries

The deep inferior epigastric artery (DIEA) originates medially from external iliac artery, immediately above the inguinal ligament, and ascends upwards between the rectus abdominis muscle and the posterior lamella of rectus sheath. It gives origin to muscular branches that perforate the rectus muscle and supplies the anterior abdominal subcutaneous fat and skin. Three different DIEA branching patterns have been described by Moon and Taylor.<sup>8</sup> Type I: a single trunk, type II: bifurcation into a medial and lateral branch (most common), and type III: three or more branches (► Fig. 1). The DIEA perforating branches are divided into medial row and lateral row perforators that supply the midline and lateral abdomen, respectively. The course of perforating arteries is divided into intramuscular, subfascial, and subcutaneous segments (► Fig. 2).<sup>9,10</sup> A pair of venae comitantes accompany each perforator artery.

The superficial inferior epigastric artery (SIEA) arises from the common femoral artery 2 to 3 cm below the inguinal ligament. According to Strauch and Yu, in 48% of the cases SIEA originates as a common trunk with the superficial circumflex iliac artery, in 17% of the cases these arteries have separate origins, and in the 35% of the cases it is absent (► Fig. 3).<sup>11-13</sup> It courses superolaterally and lies in the subcutaneous tissue anterior to rectus sheath. A larger caliber SIEA, especially with a common origin with a superficial circumflex iliac artery is favorable for microsurgical anastomosis.<sup>11,14</sup>

The anatomy of the superficial inferior epigastric vein (SIEV) is important as an extra conduit for flap venous drainage because venous congestion is an important cause of deep inferior epigastric artery perforator (DIEP) flap loss.

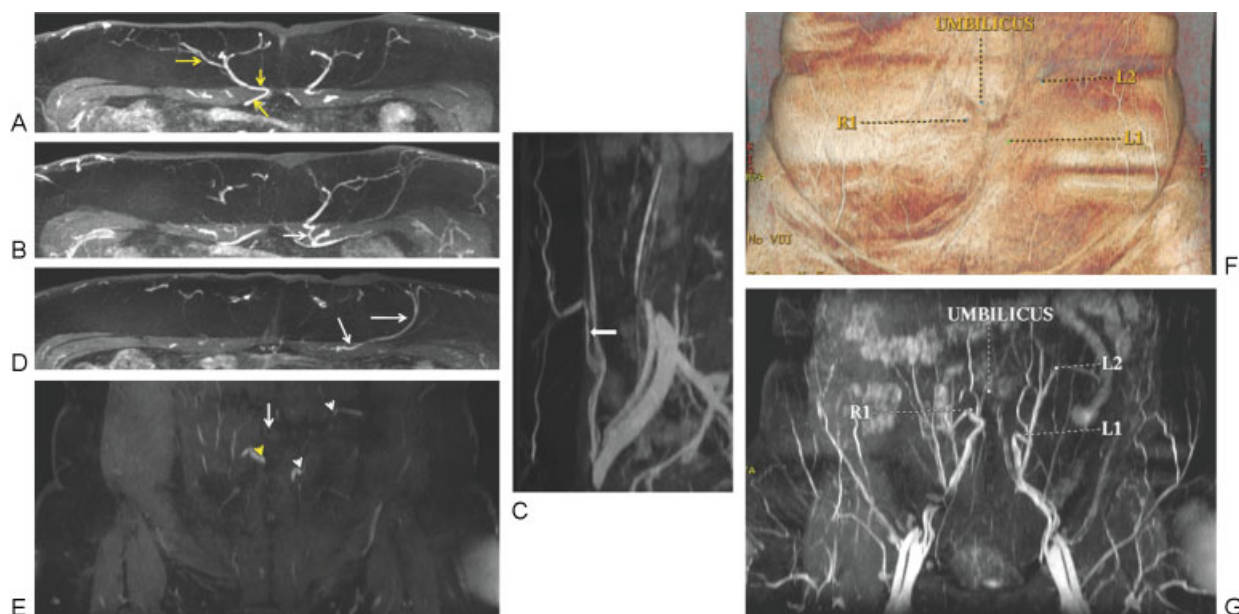


**Fig. 2** (A) Axial thick slab high-resolution equilibrium phase T1W LAVA image through the abdomen demonstrates, right side anterior abdominal wall perforator (R1) with favorable characteristics, a medial row, large caliber, septocutaneous perforator with small subfascial segment (vertical arrow) coursing around the medial border of rectus abdominis muscle (oblique arrow) thus do not require dissection of rectus abdominis muscle fibers, with good arborization pattern in subcutaneous tissue (horizontal arrow). (B, C) Axial and coronal thick slab high-resolution equilibrium phase LAVA image and its sagittal reformation demonstrates, a medial row, good caliber left side anterior abdominal wall perforator (L1) with good subcutaneous arborization pattern but, tortuous (2B, arrow) and long (2C, arrow) intramuscular course making it unfavorable. (D) Axial thick slab high-resolution equilibrium phase LAVA image through abdomen demonstrates left side anterior abdominal wall perforator (L2) (horizontal arrow), a lateral row, good caliber perforator with good subcutaneous arborization pattern but, oblique intramuscular course (oblique arrow) making it unfavorable. (E) Thick slab coronal reformation of high-resolution equilibrium phase LAVA image demonstrates the three deep inferior epigastric perforating arteries at site where they perforate through the superficial fascia with respect to umbilicus stalk (large white arrow). The left side perforators (white small arrows) perforate through the rectus muscle, while the right side perforator (arrow heads) course around the medial border of right rectus muscle. (F) Three-dimensional volume-rendered image demonstrating surface display of perforator coordinates at the level where they perforate through superficial fascia, with respect to umbilicus. (G) Thick slab coronal MIP image demonstrating position of perforators with respect to the underlying deep inferior epigastric arteries. LAVA, liver acquisition with volume acquisition; MIP, minimum intensity projection.

The SIEV lies superficial to the Scarpa fascia and communicates with the deep inferior epigastric vein through perforator venae comitantes. The communication can be direct or indirect and of varying diameter (→ Fig. 4).<sup>15,16</sup>

### Superior and Inferior Gluteal Arteries

The superior and inferior gluteal arteries (SGA and IGA) are terminal branches of posterior division of internal iliac artery. After exiting pelvis through the greater sciatic foramen, the SGA passes superior and the IGA passes inferior to the piriformis muscle. The SGA along with supplying gluteus medius, perforates through the gluteus maximus to supply its upper half and gives branches to overlying skin and subcutaneous fat. IGA supplies the lower half of gluteus maximus and sends perforators to the overlying gluteal skin and subcutaneous fat. The superior gluteal artery perforators (SGAPs) generally course at a more direct angle and the inferior gluteal artery perforators (IGAPs) course more horizontally or obliquely as they pass through the muscle (→ Fig. 5).<sup>17,18</sup>

### Transverse Upper Gracilis and Profunda Artery Perforator Flap

The gracilis muscle, receives its blood supply from perforating branches of medial femoral circumflex artery, a branch of the

profunda femoral artery. There are considerable variations in number, diameter, and location of perforators to the gracilis muscle. Usually when there are numerous perforators, each individual perforator has a smaller diameter compared with when there are only one or two perforators (→ Fig. 6). For tiny perforators, dissection off the muscle is more difficult.<sup>19,20</sup> As the gracilis muscle tends to have tiny perforators, this muscle is often harvested together with the subcutaneous fat for the transverse upper gracilis (TUG) flap.

The profunda femoris artery enters the thigh posterior compartment and typically gives off three main perforators.<sup>21</sup> The first perforator supplies the adductor magnus and gracilis, the second and third supplies the rest of the hamstring muscles. Other septocutaneous and smaller musculocutaneous perforators are also visualized variably.

## Methods

### Magnetic Resonance Angiography for Preoperative Imaging of Perforator Flap Artery

From August 2008 to August 2013 we have performed over 400 MRA examinations for preoperative imaging of perforator flaps for breast reconstruction. Our MRA protocol optimization is driven by on-going feedback from plastic surgeons.

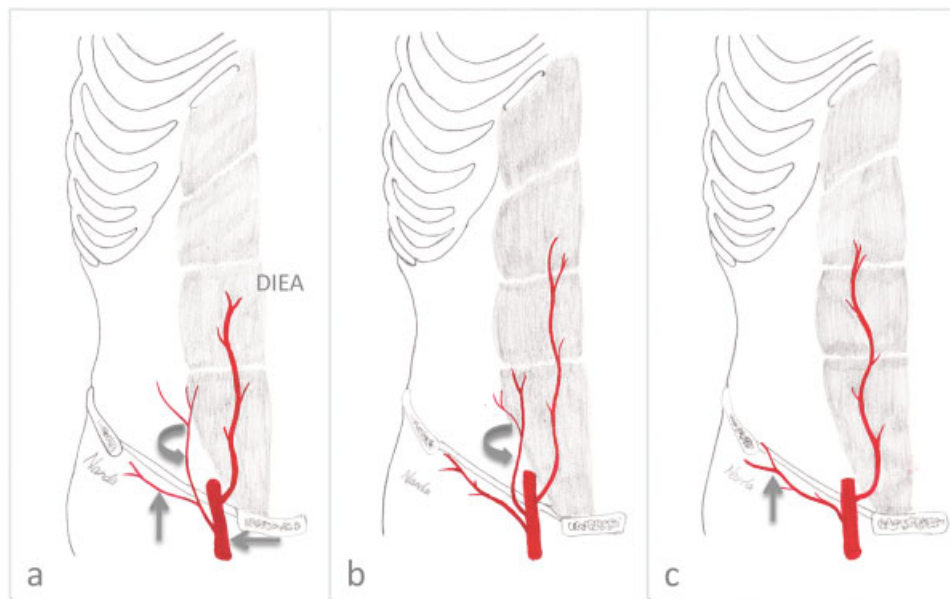


**Fig. 3** Diagrammatic illustration (frontal view) demonstrates the three common variants of superficial inferior epigastric artery (SIEA, curved arrow) anatomy: common origin with the superficial circumflex iliac artery (vertical straight arrow), arising from the common femoral artery (horizontal straight arrow) just below the inguinal ligament (A), separate origin (B), and absence (C).

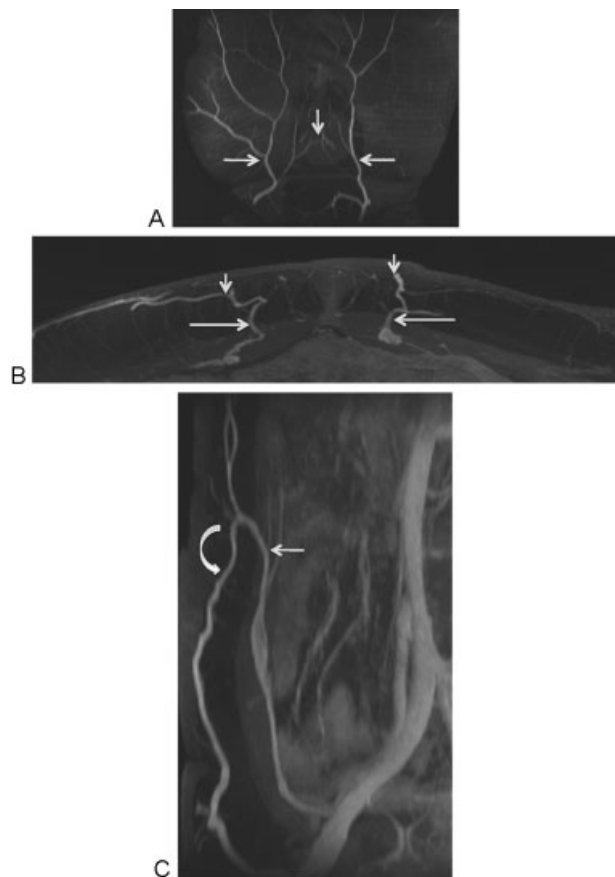


**Fig. 4** Anterior abdominal superficial venous anatomy. (A) Thick slab coronal reformation of high-resolution equilibrium phase LAVA demonstrates SIEV (horizontal arrow). Note the midline cross-over of the venous flow (vertical arrow). (B) Axial thick slab high-resolution equilibrium phase LAVA and its sagittal reformation (C) demonstrates communication between deep inferior epigastric venae comitantes (horizontal arrows) and SIEV (vertical arrow in [B] and curved arrow in [C]). LAVA, liver acquisition with volume acquisition; SIEV, superficial inferior epigastric veins.

At present, we perform MRA at 1.5 T (GE signa HDx 15.0, GE Healthcare, Waukesha, WI) for all patients who elect to undergo breast reconstruction. CTA is performed only when MRA is contraindicated or when the patient has severe claustrophobia.

Imaging in prone position has several advantages. For DIEP, prone positioning reduces respiratory motion in the anterior subcutaneous fat and allows longer, higher resolution scans with more thin slices covering a large anatomic area. The location at which the perforators exit the anterior rectus fascia in relation to the umbilical stalk's attachment to anterior rectus fascia is unaffected by the prone position because fascia is a stable structure. For SGAP and IGAP, prone positioning avoids distortion of the curved shape of the buttock and preserves the natural position of inferior gluteal crease. For these reasons, imaging in the prone position allows surgeons to accurately identify the abdominal and gluteal perforators.<sup>7</sup> Posterior thigh perforator imaging is relatively unaffected by patient position.

Phase encoding is set to right-left to ensure that breathing and peristalsis motions do not create ghosting artifacts over the anterior abdominal fat. Eliminating ghosting from bowel peristalsis is particularly important due to strong mucosal enhancement by blood pool magnetic resonance imaging (MRI) contrast agents. We routinely give 0.5 mg glucagon intravenously just before injecting contrast media. We prefer a lower flip angle (15 degrees) combined with fat suppression for MRA to delineate the fat-muscle boundary and intramuscular perforator course for guiding perforator dissection. One of the limitations with MRI can be inhomogeneous fat suppression at the edge of field of view, especially in patients with large body habitus. This problem can be addressed by using the two-point Dixon method for separation of fat and water signals.



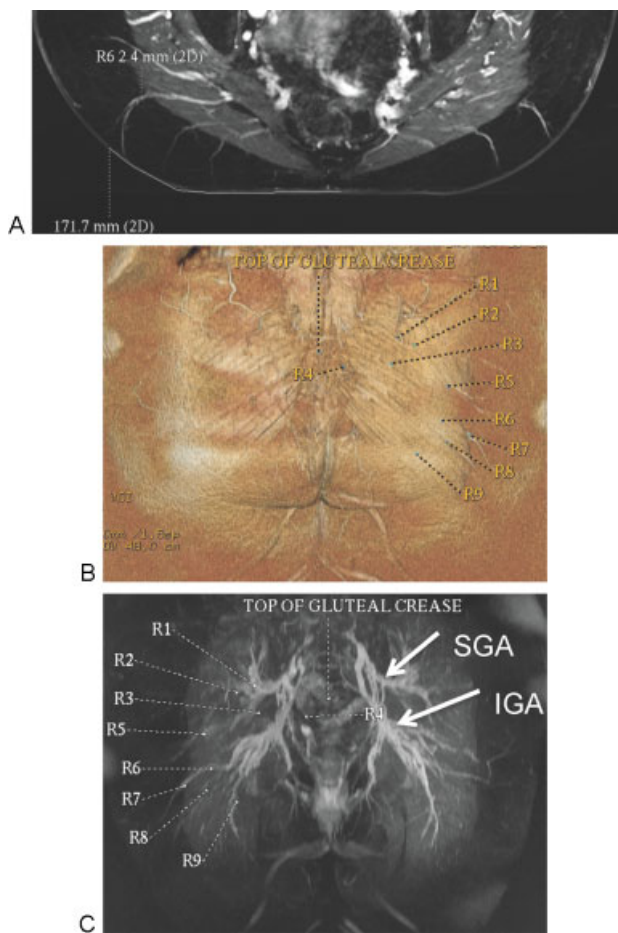


**Fig. 5** (A) Axial high-resolution equilibrium phase LAVA image through gluteal region demonstrates, gluteal artery perforator (2.4 mm in diameter, at the site where it perforates superficial fascia). The curved horizontal white line along the skin surface reveals the horizontal distance of perforator (171.7 mm) from the midline. The lateral most point of curved white line is where the surgeon places the Doppler probe and skin mark to confirm perforator artery location before dissection. (B) 3D volume-rendered image of gluteal region demonstrates surface marking of several perforators with respect to landmark, the top of midline gluteal crease. (C) 3D MIP image displaying position of perforators with respect to underlying superior and inferior gluteal arteries. 3D, three-dimensional; LAVA, liver acquisition with volume acquisition; MIP, minimum intensity projection.

At our center, we routinely inject 10 mL of gadofosveset trisodium, a blood pool MRI contrast agent. It is a gadolinium chelate that reversibly binds to serum albumin with approximately 90% binding fraction, and effectively stays within the blood pool with a relatively long redistribution half-life of 28 minutes.<sup>22</sup> It has high T1 relaxivity so that a fourfold lower molecular dose compared with other gadolinium chelates confers greater vascular enhancement. This low dose virtually eliminates the risk of nephrogenic systemic fibrosis.<sup>23</sup> Zou et al have demonstrated that gadofosveset improves vessel-to-muscle contrast ratio and vessel sharpness, mainly due to preferential enhancement of vessels compared with muscle derived from blood pool distribution of gadofosveset. Using this blood pool contrast agent permits high-resolution abdomen, buttock, and upper thigh imaging in a single MRI

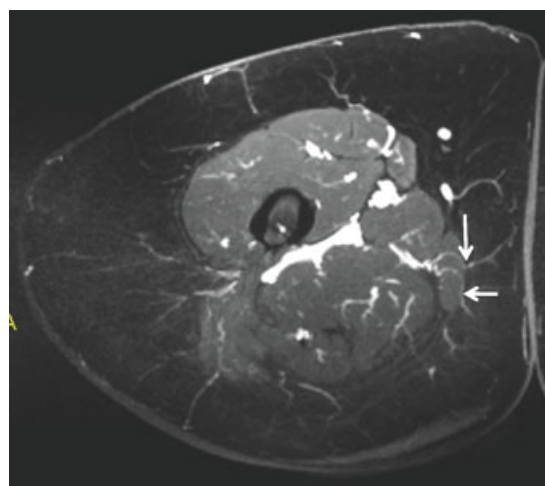


**Fig. 6** Axial high-resolution equilibrium phase LAVA through upper thigh region demonstrates a pair of gracilis muscle perforators (arrows) supplying medial subcutaneous tissue of the thigh. LAVA, liver acquisition with volume acquisition.

examination to assess all available donor sites for perforator flap breast reconstruction (i.e., DIEP, SIEA, profunda femoral artery perforator [PAP], SGAP, IGAP, TUG, and lumbar artery perforator flap).

### Magnetic Resonance Angiography Technique

Patients remove all clothing including undergarments to avoid skin and subcutaneous fat distortion from elastic bands or metal artifacts. Vitamin E capsules are placed as reference points at the top of the buttock crease and on any surgical scars. The surface landmark, patient positioning, and anatomic coverage used for different types of PFs are described in **Table 1**.

After acquiring a three plane localizer, axial, and coronal T2-weighted single shot fast spine echo images are acquired to screen for unexpected pathology and to help characterize any lesions detected on postgadolinium scans. As most of these patients have history of breast cancer, unsuspected metastatic disease may be detected: 4% of cases in our experience. These sequences are also helpful to confirm the central position of umbilicus in prone position. A transverse pre- and postcontrast arterial phase three-dimensional liver acquisition with volume acquisition (3D LAVA) sequence is acquired with imaging parameters of: TR/TE/flip = 3.9/1.9/15, bandwidth = 125 kHz, slice thickness = 3 mm reconstructed at 1.5 mm intervals using twofold zero interpolation (ZIP2), matrix = 512 × 128 to 256, parallel acceleration factor = 2. Precontrast imaging is important to determine adequacy of fat suppression. Central frequency and shim field of view can be adjusted as necessary to ensure effective fat suppression over the subcutaneous tissues of interest if Dixon fat/water separation is not available. If Dixon fat/water separation is available, for example, LAVA flex, then the echo times should be set to as close to in and out of phase as possible. The arterial phase imaging is bolus tracked by automated triggering (smartprep) or MR-fluoroscopy and scanning is initiated

**Table 1** Landmark, patient position, anatomic coverage, and specific comments for various types of perforator flaps

Flap	Landmark	Position	Coverage	Report should include
DIEP/SIEA	Umbilicus for both SI and RL coordinates	Prone	5 cm above umbilicus to pubic symphysis, ensuring coverage of origins of DIEA and SIEA	DIEA and SIEA branching pattern
				Identification of SIEV, its diameter and communication with deep venous system
				Horizontal distance of SIEV from midline, 10 cm and 12 cm inferior to umbilicus
SGAP/IGAP	Top of midline gluteal crease for SI coordinates and manual tracing along the gluteal surface from midline for RL coordinates	Prone	5 cm above top of midline gluteal crease to complete buttocks inferiorly	Gluteal fat pad thickness measured at top of crease, inferior gluteal crease and a midpoint
PAP	Inferior gluteal crease for SI coordinates and straight line along medial border of thigh for RL coordinates	Prone	Midgluteal region to 12 cm below inferior gluteal crease	Posterior thigh fat pad thickness
TUGP	Pubic symphysis for both SI and RL coordinates	Supine	Pubic symphysis to 15 cm below it	

Abbreviations: DIEA, deep inferior epigastric artery; DIEP, deep inferior epigastric perforator flap; IGAP, inferior artery perforator flap; LAP, lumbar artery perforator flap; PAP, profunda artery perforator flap; RL, right-left; SGAP, superior gluteal artery perforator flap; SI, superior-inferior; SIEA, superficial inferior epigastric artery; TDAP, thoracodorsal artery perforator flap; TUGP, transverse upper gracilis perforator.

after arrival of contrast in the abdominal aorta with breath holding on inspiration. A standard 10 mL volume of blood pool MRI contrast agent followed by 20 mL of normal saline is injected at rate of 1 mL/s. Hand injecting is preferred especially if there is a tenuous intravenous, because approximately one-third of patients may experience some sensation at the injection site or in the pelvis related to the ionic gadofosveset. A nearby comforting person performing the injection also helps the patient to hold still during the arterial phase of the injection. The K-space is mapped sequentially with the absolute center of K-space collected in the middle of scan, which is about 20 seconds after bolus detection for 35 second scan duration with a 5-second pause for breath holding instruction. This is important to provide time for the contrast to reach and fill perforator arteries. However, only the largest perforator arterial/vein bundles are adequately seen on this sequence. This is followed by equilibrium phase transverse 3D LAVA at higher resolution without parallel imaging using following parameters: TR/TE/flip = 4/1.9/15, matrix = 512 × 512 × (172 to 240), bandwidth = 125 kHz, slice thickness = 3 mm reconstructed at 1.5 mm intervals using ZIP2. Phase encoding is set to the right-left direction. This is the primary sequence utilized to generate reconstructions and create reports and also serve as a reference for the plastic surgeons. It is acquired with free breathing and typically requires 3 to 5 minutes acquisition duration with 0.9 × 0.9 × 3 mm acquired voxel dimension and 0.9 × 0.9 × 1.5 mm reconstructed voxel dimensions. Thereafter, a lower resolution coronal and sagittal plane LAVA is acquired with acquisition matrix of 512 × 256 and 512 × 224, respectively, in a single breath hold and parallel acceleration factor of 2 to evaluate internal organs.

First, the planned donor site is imaged, followed by a single high spatial resolution equilibrium phase imaging of other potential donor sites using free breathing 3D LAVA sequence described above. A typical complete perforator flap MR examination, including abdomen, buttocks and upper thigh, takes approximately 45 minutes.

### Postprocessing and Image Interpretation

After screening axial and coronal single shot fast spine echo images for unexpected pathologies, the arterial phase images are reviewed to determine number of perforators available and to look for any enhancing lesions. High spatial resolution equilibrium phase images are used for final perforator evaluation, as perforators are best visualized on these images. The equilibrium phase series is loaded on a computer workstation (GE Advantage Windows 4.4, GE Healthcare). Coronal, sagittal, and surface rendered reformatted images are generated (► Fig. 2). The user identifies the reference point and each candidate perforator artery. It is important to note that with blood pool MRA images; there is both venous and arterial enhancement. Thus, "perforator" is generally referred to the artery-vein bundle. The diameter and exit site of each perforator where they pierce superficial fascia and enter into subcutaneous fat is noted. The superior/inferior and right/left distance of each perforator exit site relative to the reference point is calculated. The intramuscular course and length of each perforator is measured to predict vascular pedicle length. Finally, a predicted flap volume is calculated on the same workstation assuming an elliptical geometry and the full abdominal subcutaneous fat thickness on a slice-by-slice basis (► Fig. 7).

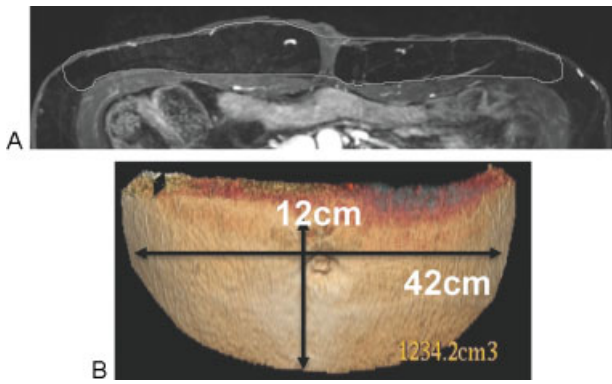


**Fig. 7** DIEP perforator flap volume estimation procedure. (A) Axial high-resolution equilibrium phase LAVA images are used to calculate perforator flap volume. Manual tracing is used to trace full thickness of anterior abdominal subcutaneous fat, a vertical distance of 12cm, starting few centimeters above umbilicus to lower down and a horizontal distance of 42 to 46 cm is covered. It is superimposed over 3D volume-rendered image, which is then cropped in an elliptical shape (B) and the volume of the simulated flap is calculated using computer software. 3D, three-dimensional; DIEP, deep inferior epigastric artery perforator; LAVA, liver acquisition with volume acquisition.

Coordinates identifying the location of the perforating arteries on the axial images are superimposed and displayed on volume-rendered 3D reconstructed image and coronal 3D minimum intensity projection image (►Fig. 2). These images and coordinates are invaluable for the plastic surgeon to locate the perforator arteries during preoperative surface making and intraoperatively. Anatomic detail that needs to be reported specific to the type of perforator flap of interest is given in ►Table 1.

## Results

In our practice, anterior abdominal wall tissue is the most commonly used donor site for perforator flap breast reconstruction and DIEP are the most commonly used vascular pedicle. In our experience, there are always at least three to four good DIEP perforators on either side of the abdomen, usually, the left side perforators are larger in caliber than the right side perforators.

In patients with insufficient anterior abdominal wall fat or distorted vascular anatomy due to previous abdominal surgery, the thigh and buttock are the next most commonly used donor sites. A thigh flap, based on the PAP flap has become the second most used flap in our institution. At present, the ratio of PAP flap to gluteal flaps (SGAP/IGAP) performed at our institute is 9:1, indicating an increasing surgical preference for the posterior thigh harvest site.<sup>24</sup> Dissection is easier for PAP flaps, it produces a longer pedicle, and there is a favorable cosmetic result achieved by tucking the PAP harvest site scar into the buttock crease.

Usually there are at least one to two good PAP perforators on either medial thigh. Medial perforators have a generous length and can be dissected with supine frog-leg positioning so the patient does not need to be flipped over in the

operating room between harvesting at the donor site and performing the breast reconstruction (►Fig. 8).<sup>21</sup> Lateral perforators may be larger in caliber but are rarely used because their close proximity to the femur requires dissection off the periosteum which can be challenging.

In our experience, MRA is not reliable for the assessment of SIEA. Only in 10% of the MRA studies, SIEA is visualized and is usually small in diameter making microsurgical anastomosis with internal mammary artery (IMA) difficult and prone to thrombosis. In addition, it is located on the inferior edge of the flap and may not well perfuse the more medial or central fat on the abdomen potentially leading to fat necrosis with possible loss of areas of the flap. Therefore, the SIEA flap is only used when DIEP vessels are not available in our practice.

MRA imaging also screens for metastatic disease which was found in 4% of our patients on a retrospective analysis done on 120 patients at Weill Cornell Medical College from October 2011 to November 2012.<sup>24</sup> The T2-weighted and contrast enhanced T1-weighted sequences are useful for detection and characterization of metastatic lesions.

## Discussion

Preoperative perforator flap donor site imaging facilitates developing a surgical strategy and backup plans beforehand, thereby decreasing operative time, reducing intraoperative complications, and improving outcomes. It provides an opportunity to select the best available perforator and plan the flap design accordingly. At present, various imaging modalities are available for preoperative imaging for perforator flap breast reconstruction. Advantages and disadvantages of each are described in ►Table 2.<sup>5,6</sup> Although, CTA is widely used for imaging perforator arteries,<sup>9</sup> recent concerns over CTA radiation exposures, which can be as high as 70 mSv for perforator CTA,<sup>25</sup> have led to reductions in CTA dose and a corresponding reduction in CTA image quality. Several studies have established comparable accuracy of MRA and CTA in preoperative perforator artery imaging.<sup>7,25–28</sup> MRA does not involve exposure to ionizing radiation or potentially nephrotoxic iodinated contrast agents. Moreover, MRA of donor sites using gadofosveset trisodium, a blood pool contrast agent provides opportunity to scan multiple donor sites in single study (►Fig. 9). At present, MRA is limited in the assessment of SIEA anatomy. However, the newer MRI techniques such as high temporal resolution LAVA spiral and two-point Dixon for fat and water separation (LAVA Flex, GE Healthcare) appear promising and may improve assessment of SIEA anatomy in the future.

A noncontrast MRA can also be performed and has been shown superior to CT for preoperative imaging of breast reconstruction with DIEP flaps as described by Masia et al. In their study of 56 patients, preoperative noncontrast MRI showed no false-positive or false-negative results with 100% predictive value in selection of the most appropriate dominant DIEA perforator.<sup>29</sup>

The cost for radiological examination varies from center to center. The Manhattan Medicare reimbursement for CTA abdomen and pelvis<sup>30</sup> with and without contrast is \$582

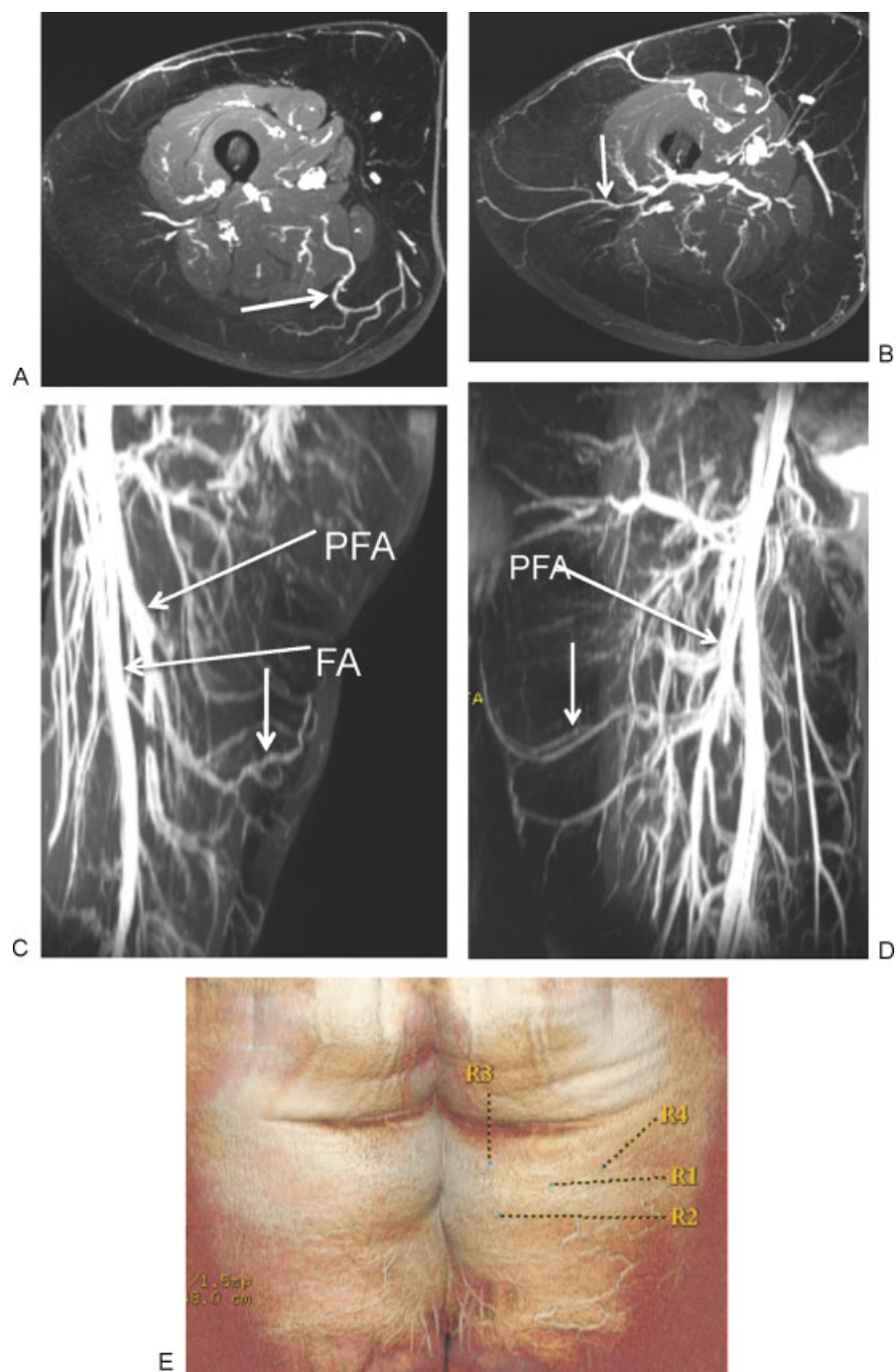


**Fig. 8** Thick slab axial high-resolution equilibrium phase LAVA through posterior thigh region (A, B) demonstrate, a good caliber medial intramuscular profunda femoral artery perforator (A, arrow) and a lateral septocutaneous profunda femoral artery perforator (B, arrow) with good subcutaneous fat arborization pattern. A medial profunda perforator is preferred over lateral one. Corresponding (C) sagittal and (D) coronal reformatted images showing position of the perforators (arrow) with respect to underlying PFA and FA. (E) A 3D volume-rendered image demonstrating surface display of perforator position with respect to landmark, inferior gluteal crease. 3D, three-dimensional; FA, femoral artery; LAVA, liver acquisition with volume acquisition; PFA, profunda femoral artery.

and MRA abdomen and pelvis with and without contrast is about one-third more. However, in our experience a good quality MRA of abdomen and pelvis using blood pool contrast agent provides high contrast and high spatial resolution imaging of multiple donor site in a single MRA examination. Therefore, in some cases when the anatomy of initially imaged donor site is unfavorable or due to lack of good perforator, it avoids a second visit to the hospital for a second examination.

#### Factors Considered while Selecting Optimal Perforator Vessel

The foremost factors determining the optimal perforator are vessel diameter, site of vessel entry into the planned flap, and its arborization pattern within the adipocutaneous tissue.<sup>7</sup> A larger diameter, central location on the proposed flap, and a pattern of arborization that suggests adequate perfusion of the tissue to be transferred is



**Table 2** Advantages and disadvantages of various modalities used for preoperative imaging of perforator flap arteries

Modality	Advantages	Disadvantages
Unidirectional Doppler	<ul style="list-style-type: none"> <li>• Portable</li> <li>• Simple to use</li> <li>• Useful tool for intraoperative evaluation to document and follow the flow of a chosen perforator during dissection</li> <li>• No IV contrast</li> <li>• Overall low cost</li> <li>• No radiation</li> </ul>	<ul style="list-style-type: none"> <li>• Time-consuming and low accuracy</li> <li>• High interobserver variability</li> <li>• No information about vessel diameter, anatomic course, and can detect only vessels &gt; 1.5 mm in diameter</li> <li>• Inability to distinguish perforators that arise from the superficial or deep system accurately</li> <li>• Failure to locate perforators that do not exit fascia perpendicularly</li> </ul>
Color duplex ultrasonography	<ul style="list-style-type: none"> <li>• Detects vessel diameter, velocity and anatomic course</li> <li>• No IV contrast</li> <li>• Overall low cost</li> <li>• No radiation</li> </ul>	<ul style="list-style-type: none"> <li>• Require highly trained technicians with good knowledge of perforator anatomy</li> <li>• Time-consuming and require patient to be one position for long time</li> <li>• Cannot produce images that surgeons can independently review and understand</li> </ul>
CTA	<ul style="list-style-type: none"> <li>• Current gold standard</li> <li>• Quick and easy to perform</li> <li>• Less dependent on body habitues</li> <li>• Accurate documentation of vessel diameter, location and course of vessels</li> <li>• Provide high-spatial resolution 2D and 3D image which surgeons can view easily and independently</li> </ul>	<ul style="list-style-type: none"> <li>• Ionizing radiation exposure</li> <li>• Risk of nephrotoxicity with contrast even in patient with normal renal function</li> </ul>
MRA (becoming increasingly popular)	<ul style="list-style-type: none"> <li>• Safer MRI blood pool contrast agent</li> <li>• No exposure to ionizing radiation</li> <li>• Accurate documentation of vessel diameter, location, and course</li> <li>• Large field of view with ability to image multiple donor site in a single study</li> <li>• Multiple acquisitions in single scan images of both arteries and veins</li> <li>• Greater muscle to vessel contrast and fat suppression, which enables visualization of small caliber vessels</li> <li>• Provides high-spatial resolution 2D and 3D image which surgeons can view easily and independently</li> </ul>	<ul style="list-style-type: none"> <li>• Longer scan time</li> <li>• Need for MR contrast agent</li> <li>• Contraindicated in patients with severe claustrophobia, pacemaker</li> </ul>

Abbreviations: 2D, two-dimensional; 3D, three-dimensional; CTA, computed tomography angiography; IV, intravenous; MRA, magnetic resonance angiography; MRI, magnetic resonance imaging.

favorable. A perforator that is > 1 mm in diameter and located in an area favorable for flap harvest is desirable (► Fig. 2). On MRI obtained during the blood pool phase of the contrast agent injection, the artery and vein are indistinguishable so the perforator diameter measurement corresponds to the artery/vein bundle. The vessel course is also important but considered a secondary factor in perforator selection. Among two vessels of similar caliber and arborization patterns, the vessel that can be dissected more easily with least trauma to muscle is selected.<sup>7</sup> Generally, several

perforators on each side need to be identified and reported by the radiologist because the best perforators may be damaged or appear differently at surgery, necessitating the availability of backup perforators. A septocutaneous perforator is a perforator that travels around the muscle. An intramuscular perforator traverses the muscle. Perforators with short intramuscular course or a septocutaneous course are preferred because dissection is easier and quicker with minimal muscle trauma (► Fig. 2). A long or tortuous intramuscular course makes dissection tedious

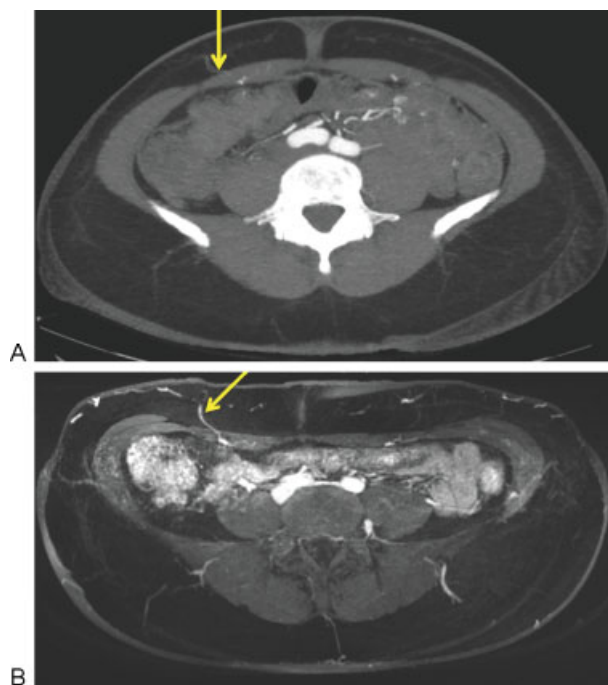


**Fig. 9** A 45-year-old woman underwent both CTA and MRA of abdomen for preoperative DIEA perforator vessel mapping. Axial thick slab CTA image through abdomen (A) demonstrates poor visualization due to poor contrast enhancement of right side DIEA perforator (arrow). A repeat MRA study was performed. Axial thick slab high-resolution equilibrium phase T1W LAVA image (B) through the abdomen demonstrates same right side DIEA perforator (arrow) with good contrast enhancement and improved visualization of intramuscular course. CTA, computed tomography angiography; DIEA, deep inferior epigastric artery; MRA, magnetic resonance angiography; LAVA, liver acquisition with volume acquisition.

and increases potential for injury to the muscle and/or perforator.

The available pedicle length is yet another factor to consider. The vessel is dissected until its origin from a major artery (e.g., external iliac artery, profunda femoral artery). Adequate vascular pedicle length and caliber facilitates tension free microanastomosis with the IMA. A pedicle length of at least 6 cm is favored.

In conclusion, MRA is an invaluable tool for preoperative imaging of perforator flap arteries for breast reconstruction. Knowledge of relevant anatomy and protocols for acquiring MRA, postprocessing, and interpretation of MRA images can help to improve surgical planning, reduce operative time and postoperative complications.

## References

- International Agency for Research on Cancer. GLOBOCAN 2008: Cancer incidence and mortality worldwide. Available at: <http://www.iarc.fr/en/media-centre/iarcnews/2010/globocan2008.php>. Accessed September 22, 2013
- Bostwick J III. Breast reconstruction following mastectomy. *CA Cancer J Clin* 1995;45(5):289–304
- Rawson AE, McClellan WT. Current concepts in breast reconstruction. *W V Med J* 2009;105(Spec No):16–22, quiz 23

- Fodor L, Bota IO, Filip CI, et al. New trends in breast reconstruction. *Chirurgia (Bucur)* 2011;106(4):485–489
- Mathes DW, Neligan PC. Current techniques in preoperative imaging for abdomen-based perforator flap microsurgical breast reconstruction. *J Reconstr Microsurg* 2010;26(1):3–10
- Mathes DW, Neligan PC. Preoperative imaging techniques for perforator selection in abdomen-based microsurgical breast reconstruction. *Clin Plast Surg* 2010;37(4):581–591, xi
- Greenspun D, Vasile J, Levine JL, et al. Anatomic imaging of abdominal perforator flaps without ionizing radiation: seeing is believing with magnetic resonance imaging angiography. *J Reconstr Microsurg* 2010;26(1):37–44
- Moon HK, Taylor GI. The vascular anatomy of rectus abdominis musculocutaneous flaps based on the deep superior epigastric system. *Plast Reconstr Surg* 1988;82(5):815–832
- Phillips TJ, Stella DL, Rozen WM, Ashton M, Taylor GI. Abdominal wall CT angiography: a detailed account of a newly established preoperative imaging technique. *Radiology* 2008;249(1):32–44
- Granzow JW, Levine JL, Chiu ES, Allen RJ. Breast reconstruction with the deep inferior epigastric perforator flap: history and an update on current technique. *J Plast Reconstr Aesthet Surg* 2006;59(6):571–579
- Fukaya E, Kuwatsuru R, Iimura H, Ihara K, Sakurai H. Imaging of the superficial inferior epigastric vascular anatomy and preoperative planning for the SIEA flap using MDCTA. *J Plast Reconstr Aesthet Surg* 2011;64(1):63–68
- Strauch B, Yu H-L. *Atlas of Microvascular Surgery: Anatomy and Operative Techniques*. New York, NY: Thieme; 2006
- Karunanithy N, Rose V, Lim AKP, Mitchell A. CT angiography of inferior epigastric and gluteal perforating arteries before free flap breast reconstruction. *Radiographics* 2011;31(5):1307–1319
- Tseng CY, Lipa JE. Perforator flaps in breast reconstruction. *Clin Plast Surg* 2010;37(4):641–654, vi–ii
- Rozen WM, Pan W-R, Le Roux CM, Taylor GI, Ashton MW. The venous anatomy of the anterior abdominal wall: an anatomical and clinical study. *Plast Reconstr Surg* 2009;124(3):848–853
- Schaverien MV, Ludman CN, Neil-Dwyer J, et al. Relationship between venous congestion and intraflap venous anatomy in DIEP flaps using contrast-enhanced magnetic resonance angiography. *Plast Reconstr Surg* 2010;126(2):385–392
- Ahmadzadeh R, Bergeron L, Tang M, Morris SF. The superior and inferior gluteal artery perforator flaps. *Plast Reconstr Surg* 2007;120(6):1551–1556
- Rozen WM, Ting JWC, Grinsell D, Ashton MW. Superior and inferior gluteal artery perforators: In-vivo anatomical study and planning for breast reconstruction. *J Plast Reconstr Aesthet Surg* 2011;64(2):217–225
- Fansa H, Schirmer S, Warnecke IC, Cervelli A, Frerichs O. The transverse myocutaneous gracilis muscle flap: a fast and reliable method for breast reconstruction. *Plast Reconstr Surg* 2008;122(5):1326–1333
- Kappler UA, Constantinescu MA, Büchler U, Vögelin E. Anatomy of the proximal cutaneous perforator vessels of the gracilis muscle. *Br J Plast Surg* 2005;58(4):445–448
- Allen RJ, Haddock NT, Ahn CY, Sadeghi A. Breast reconstruction with the profunda artery perforator flap. *Plast Reconstr Surg* 2012;129(1):16e–23e
- Lauffer RB, Parmelee DJ, Dunham SU, et al. MS-325: albumin-targeted contrast agent for MR angiography. *Radiology* 1998;207(2):529–538
- Ersoy H, Jacobs P, Kent CK, Prince MR. Blood pool MR angiography of aortic stent-graft endoleak. *AJR Am J Roentgenol* 2004;182(5):1181–1186
- Thimmappa ND, Dutruel SP, Pei M, et al. Pre-operative perforator flap MRA for autologous breast reconstruction. In: *Proceedings of the 21st*

- Annual Meeting and Exhibition of International Society for Magnetic Resonance in Medicine; April 20–26, 2013; Salt Lake City, UT
- 25 Zou Z, Kate Lee H, Levine JL, et al. Gadofosveset trisodium-enhanced abdominal perforator MRA. *J Magn Reson Imaging* 2012;35(3):711–716
  - 26 Vasile JV, Newman T, Rusch DG, et al. Anatomic imaging of gluteal perforator flaps without ionizing radiation: seeing is believing with magnetic resonance angiography. *J Reconstr Microsurg* 2010;26(1):45–57
  - 27 Newman TM, Vasile J, Levine JL, et al. Perforator flap magnetic resonance angiography for reconstructive breast surgery: a review of 25 deep inferior epigastric and gluteal perforator artery flap patients. *J Magn Reson Imaging* 2010;31(5):1176–1184
  - 28 Chernyak V, Rozenblit AM, Greenspun DT, et al. Breast reconstruction with deep inferior epigastric artery perforator flap: 3.0-T gadolinium-enhanced MR imaging for preoperative localization of abdominal wall perforators. *Radiology* 2009;250(2):417–424
  - 29 Masia J, Kosutic D, Cervelli D, Clavero JA, Monill JM, Pons G. In search of the ideal method in perforator mapping: noncontrast magnetic resonance imaging. *J Reconstr Microsurg* 2010;26(1):29–35
  - 30 CodeMap. 2013 Medicare physician fee schedule reimbursement. Available at: <https://www.codemap.com/ge/index.cfm?cat=5&subcat=27>. Accessed December 22, 2013